Validation of the *k*-filtering technique for a signal composed of random-phase plane waves and non-random coherent structures

O. W. Roberts, X. Li, and L. Jeska

Department of Mathematics and Physics, Aberystwyth University, Aberystwyth, SY23 3BZ, UK

Correspondence to: O. W. Roberts (o.wyn.roberts@gmail.com)

Abstract. Recent observations of astrophysical magnetic fields have shown the presence of fluctuations being wave-like (propagating in the plasma frame) and those described as being structure-like (advected by the plasma bulk velocity). Typically with single-spacecraft missions it is impossible to differentiate between these two fluctuations, due to the inherent spatio-temporal ambiguity associated with a single point measurement. However missions such as Cluster which contain multiple spacecraft have allowed for temporal and spatial changes to be resolved, using techniques such as *k* filtering. While this technique does not assume Taylor's hypothesis it requires both weak stationarity of the time series and that the fluctuations can be described by a superposition of plane waves with random phases. In this paper we test whether the method can cope with a synthetic signal which is composed of a combination of non-random-phase coherent structures with a mean radius *d* and a mean separation λ, as well as plane waves with random phase.

1 Introduction

Understanding plasma physics processes in three dimensions is one of the major goals of the Cluster mission (Escoubet et al., 2001). The tetrahedral arrangement of the four identical spacecraft allows the disentanglement of temporal and spatial changes unambiguously in three dimensions. This property is essential to be able to distinguish between the two competing ideas for plasma heating in astrophysical plasmas: that of wave damping and that of dissipation in coherent structures. In this regard, single-spacecraft measurements can be quite limiting, and Taylor's hypothesis needs to be invoked (Taylor, 1938).

The *k*-filtering technique (Pinçon and Lefeuvre, 1991) is a multi-spacecraft analysis technique, with the advantage that Taylor's hypothesis is not required. Here we use the term "*k* filtering" to refer to all techniques which are based on the same mathematics (Pinçon and Motschmann, 1998), e.g. the wave-telescope technique (Neubauer and Glassmeier, 1990) or the multi-point signal resonator technique (Narita et al., 2011). The method takes the magnetic field (or magnetic and electric fields) measurements from the four spacecraft and is able to determine the full three-dimensional power spectral density $P(\omega, \mathbf{k})$. A filter bank approach is used and the measured signals are filtered such that the only powers that pass through the filter correspond to a plane wave at the chosen frequency ω, and wave vector $\mathbf{k}$, with all other powers in the signal being eliminated. The filtering can be performed for a number of points in wave space $\mathbf{k} = (k_x, k_y, k_z)$ and a fully three-dimensional estimation of the power spectral density $P(\omega, \mathbf{k})$ in wave number space can be constructed.

The method itself has been tested extensively for a superposition of plane waves with random phases (e.g. Pinçon and Lefeuvre, 1991, 1992; Motschmann, 1996; Pinçon and Motschmann, 1998; Sahraoui et al., 2010), and the effects of noise, time synchronisation inaccuracies, spacecraft position inaccuracies and poor tetrahedral configurations are well understood. However, the random-phase approximation is an assumption that has not been discussed thoroughly. The key assumption for this method is that the measured fluctuations can be described as a superposition of plane waves *with random phases* (Capon, 1969; Pinçon and Lefeuvre, 1991, 1992; Motschmann et al., 1998; Tjulin et al., 2005). Here the term "random-phase plane waves" refers to waves with randomised (non-fixed) phase difference at each consecutive wave period. Practically, for the application of the *k*-filtering

method, this requires that waves with different wave vectors be incoherent at each frequency.

The *k*-filtering method has been used in several near-Earth plasma environments with input coming exclusively from magnetic field measurements (e.g. the magnetosheath, the foreshock and the solar wind; Glassmeier et al., 2001; East-wood et al., 2003; Sahraoui et al., 2003, 2004; Roberts et al., 2013), and has also been applied using a combination of both magnetic and electric field measurements (Tjulin et al., 2005, 2008).

A recent study which applied the *k*-filtering technique to the solar wind was performed by Roberts et al. (2013), in which it was concluded that the solar wind may be populated by linear kinetic Alfvén waves (KAWs), as well as coherent structures which are advected by the bulk velocity (e.g. monopolar Alfénic vortices (Alexandrova et al., 2006; Alexandrova, 2008), pressure balanced structures (Burlaga and Ogilvie, 1970)) or those propagate with a small velocity $v \ll V_{\mathrm{sw}}$ in the plasma rest frame (e.g. dipolar Alfvén vortices; Petviashvili and Pokhotelov, 1985, 1992). In other plasma environments such as the magnetosphere, bulk velocity is typically smaller than the solar wind. In this case we may expect that fluctuations have a significant component of the velocity to be along the direction of the magnetic field along in addition to the typical velocity due to the advection. This study concluded that techniques such as *k* filtering may need to be further validated for analysis of a signal which is composed of a superposition of coherent structures and random-phase plane waves. In relation to the signal we use the term "coherent structure" to denote a coherent wave packet, i.e. a coherent signal windowed by an envelope of limited extension. Coherent structures are characterised by a radius and a mean spacing between them. It is important to note that, within the radius of a structure, the variation of the signal (magnetic field) is known and the phases are not random. This makes it similar to a coherent wave packet. However with respect to other structures they are likely to be incoherent, and a key goal of this work is to determine the effect of coherency on the determination of the power of waves or structures when the *k*-filtering technique is adopted.

Here we quote the comments of Pinçon and Lefeuvre (1991) when the *k*-filtering method was first designed: "Measurements of the electric and/or magnetic field in space plasmas commonly show fluctuations in time and/or space on all observed scales; such fluctuations are mostly random in appearance and therefore are considered as turbulent phenomena". While we would expect waves in a turbulent plasma to have random phases, it is unclear whether this is satisfied for a population of coherent structures being advected past the spacecraft or for a signal with a coexistence of random-phase plane waves and coherent structures (including short-lived coherent wave packets). The paper is also motivated by studies in which discrete waves were indeed observed in the solar wind (Jian et al., 2009, 2010) and in which discrete

waves were able to survive in a turbulent environment for a limited time, at least theoretically (Ghosh et al., 2009).

The goal of this work is to provide such a validation for the technique using synthetic magnetic field data. The *k*-filtering method will be presented in Sect. 2. Then we will present the various signals which we will input to the method, and how they were defined, in Sect. 3, followed by the results and conclusions.

2   The *k*-filtering method

Here we will provide a brief introduction to *k* filtering, following the notation given in Pinçon and Motschmann (1998) and Tjulin et al. (2005). Regarding the array of detectors, in our case we have the Cluster spacecraft and the magnetometer measurements, which yield 12 time series (in our case four satellites yield three measurements each). We can represent our data as the following vector:

$$\mathbf{A}(\boldsymbol{r}_{\alpha}, t) = \begin{pmatrix} \mathrm{A}(\boldsymbol{r}_1, t) \\ \vdots \\ \vdots \\ \mathrm{A}(\boldsymbol{r}_{12}, t) \end{pmatrix}. \tag{1}$$

These time series are then transformed into frequency space by using a windowed Fourier transform (Eq. 2). The size of the window determines the frequency resolution. When we have a window of a single data point (window size is zero), no frequency information can be obtained. In the other extreme case where we only have one window for an interval, we are unable to resolve any temporal variations (Motschmann, 1996). Typically windows of 1024 points (which corresponds to 45 s for nominal mode Cluster FGM data sampled at 22 Hz; Balogh et al., 2001) are used (Sahraoui et al., 2003, 2006). This corresponds to a frequency resolution of ~ 0.024 Hz (Sahraoui et al., 2003), suitable for studying inertial and dissipation scales in the solar wind. It should also be noted that a key limitation due to the use of a windowed Fourier transform is the requirement that the time series be at least weakly stationary so that the goal of achieving ensemble average, a key requirement of the *k*-filtering method, can be realised by using time averages. This is an important restriction when selecting intervals for analysis. Intervals are chosen such that the magnetic field time series are devoid of shocks, discontinuities or any trends so that the quality of the results are not impaired.

$$\mathbf{A}(\boldsymbol{r}_{\alpha}, \omega) = \begin{pmatrix} \mathrm{A}(\boldsymbol{r}_1, \omega) \\ \vdots \\ \vdots \\ \mathrm{A}(\boldsymbol{r}_{12}, \omega) \end{pmatrix} \tag{2}$$

This is a 12×1 column vector containing three components of the Fourier-transformed magnetic field for four satellites.
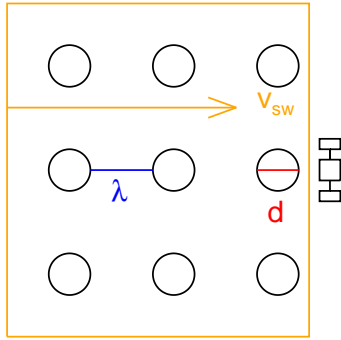
Figure 1. Schematic of a number of structures with a mean separation λ and diameter d (or thickness) of the structures. These are being advected over the spacecraft with the solar wind bulk velocity.

From this the correlation matrix can be found, which is the ensemble average of the matrix product of the Fourier transformed time series, and its Hermitian adjoint (transposed and complex conjugated denoted by the superscript plus) can be written as

$$\mathbf{M}(\omega) = \langle (\mathbf{A}(\omega)\mathbf{A}^+(\omega)) \rangle. \tag{3}$$

If a time series is weakly stationary and spatially homogeneous, then we can replace the ensemble average in Eq. (3) with a time average. This is an important limitation of the method, as the time series is not stationary; for example, if there are trends in the data, then the ensemble average and the time average will not be the same, and we will not be able to use a time average.

We now need to constrain the data such that no unphysical results are obtained. This is done by ensuring that the distances between the spacecraft (and the associated phase difference) are accounted for in the estimation from k filtering. To account for the relative spacecraft positions and the differences in phase in relation to this, we define a matrix $\mathbf{H}$,

$$\mathbf{H}(\boldsymbol{k}) = \begin{pmatrix} \mathbf{I}e^{i\boldsymbol{k}_1\boldsymbol{r}_1} \\ \vdots \\ \vdots \\ \mathbf{I}e^{i\boldsymbol{k}_4\boldsymbol{r}_4} \end{pmatrix}, \tag{4}$$

where $\mathbf{I}$ is the identity matrix. When working solely with magnetic field data, a second condition is also used, where we enforce the solution to be divergence-free. When using both electric and magnetic fields Faraday's law can be used instead to constrain our solutions. We can ensure that the divergence-free condition is satisfied by the estimated solutions by making $\boldsymbol{k} \cdot \delta\mathbf{B} = 0$, and this is implemented by using the constraining matrix $\mathbf{C}$, where the matrix is given by (Pinçon and Motschmann, 1998)

$$\mathbf{C}(\omega, \boldsymbol{k}) = \mathbf{I} + \frac{\boldsymbol{k}\boldsymbol{k}^+}{|\boldsymbol{k}|^2}. \tag{5}$$
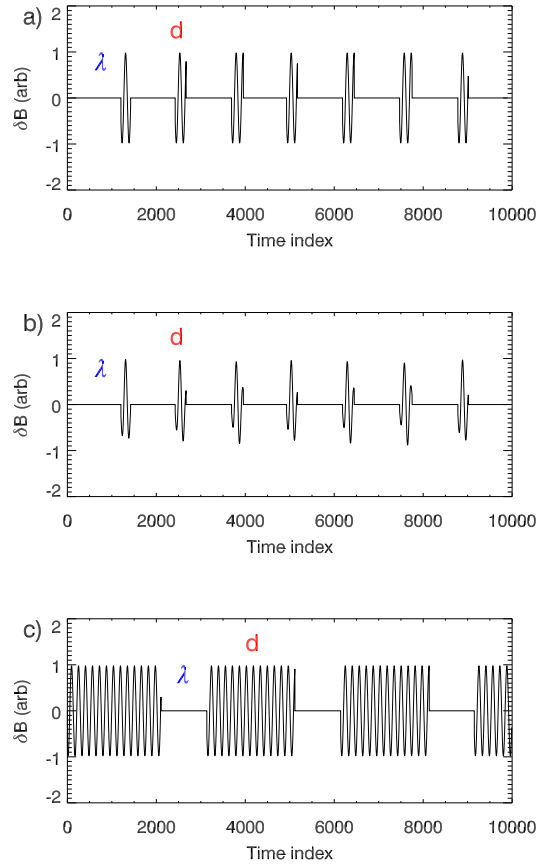
Figure 2. (a) Typical time series made up of structures with a mean spacing $\lambda = 1000$ time steps and $d = 250$ time steps. **(b)** Time series of structures which have been modulated by a Gaussian envelope. **(c)** Time series with $\lambda = 1000$, $d = 2000$. The values of λ and d vary with Poisson statistics, where the mean value is equal to the variance.

It follows that the full k-filtering equation is given by

$$P(\omega, \boldsymbol{k}) = Tr\left\{ \left[\mathbf{C}^+(\omega, \boldsymbol{k})\mathbf{H}^+(\boldsymbol{k})\mathbf{M}^{-1}(\omega)\mathbf{H}(\boldsymbol{k})\mathbf{C}(\omega, \boldsymbol{k}) \right]^{-1} \right\}. \tag{6}$$

3 Simulated magnetic field data

To simulate magnetic field data, we begin with a superposition of eight plane waves with equal power as described by

$$\delta\mathbf{B} = \sum_{i=1}^{8} \left[\frac{-k_{iy}}{k_i}\boldsymbol{e}_x + \frac{k_{ix}}{k_i}\boldsymbol{e}_y \right] [\sin(\boldsymbol{k}_i \cdot \boldsymbol{r} - \omega_i t - \phi_i) + N_i], \tag{7}$$

where $\boldsymbol{k}_i = k_{ix}\boldsymbol{e}_x + k_{iy}\boldsymbol{e}_y$ is the wave vector of the ith wave, ω is the angular frequency, $k_i = \sqrt{k_{ix}^2 + k_{iy}^2}$ is the wave number defined, and $\boldsymbol{e}_x$ and $\boldsymbol{e}_y$ are two unit vectors along the x and y axis in a Cartesian coordinate system. A uniform background magnetic field can be in any direction. N_i is the
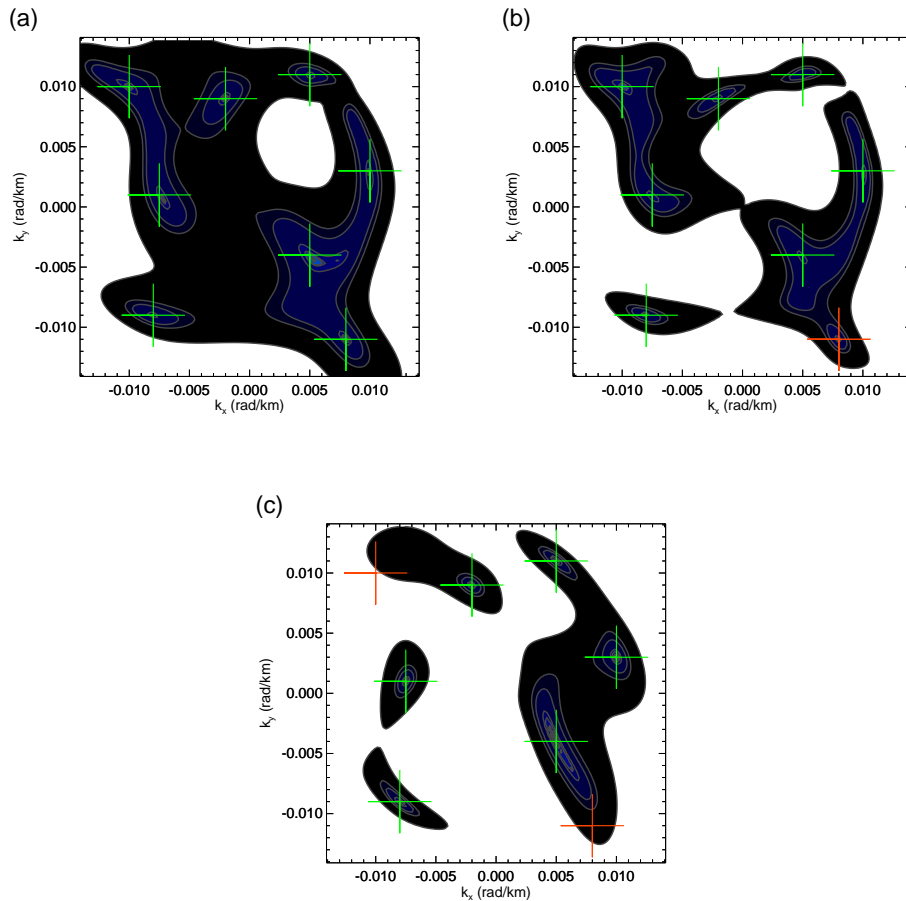
Figure 3. Estimated $P(\omega, \boldsymbol{k})$ for **(a)** eight random-phase plane waves, **(b)** seven random-phase plane waves and one fixed-phase plane wave (red cross), **(c)** six random-phase plane waves and two fixed-phase plane waves. The contours denote 0.1, 0.5, 1, 10, 25, 30, 50, 80 and 90 % of the maximum power, which cover the large range of powers estimated from the method well.

noise term, which is set at the 1 % level and is required to ensure that there is a solution to the k-filtering method (Pinçon and Lefeuvre, 1991). Here all waves are given a frequency of 0.2 Hz. The signal is divergence-free. Spacecraft are at distances $\boldsymbol{r}$ in a perfect tetrahedral configuration such that the planarity and elongation (see Robert et al., 1998, for details of the Cluster tetrahedral configuration) are $P \sim E \sim 0$. The phase term ϕ is randomised between $\pm 2\pi$ in each wave period in the case of a random-phase plane wave. The randomisation process is a "jump" in the phase and not a continuous variation as a function of time $\phi(t)$. A continuous variation in the phase is not expected over short timescales. For a series of unrelated wave trains made up of wave packets (or a number of coherent structures) we would expect the phase to jump with each new wave packet in the train. We do not investigate changes in phase in the spatial domain, since these are assumed to be small on the scales of spacecraft separation.

This gives perhaps the simplest case we can investigate of a superposition of random-phase plane waves.

We use a superposition of eight plane waves at a single frequency, since we are theoretically limited to recover $NL - 1$, waves where N is the number of spacecraft and L is the number of components we can resolve (Tjulin et al., 2005). Therefore, we are theoretically limited to 11 waves; however the resolution is too low to uniquely be able to identify more than eight waves.

To test the method we will define three different signals, and investigate the properties of the estimated power spectral density for each of the input signal. The first case we will test consists of a pure superposition of random-phase plane waves. This case has been extensively tested previously, with both electric and magnetic field measurements (Pinçon and Motschmann, 1998), as well as only magnetic field measurements (Motschmann, 1996).

The next case we will test is that of a signal composed of both random-phase plane waves and non-random-phase plane waves. This is implemented as a result of some of the waves in Eq. (7) having a constant phase, so they are not randomised in each wave period.
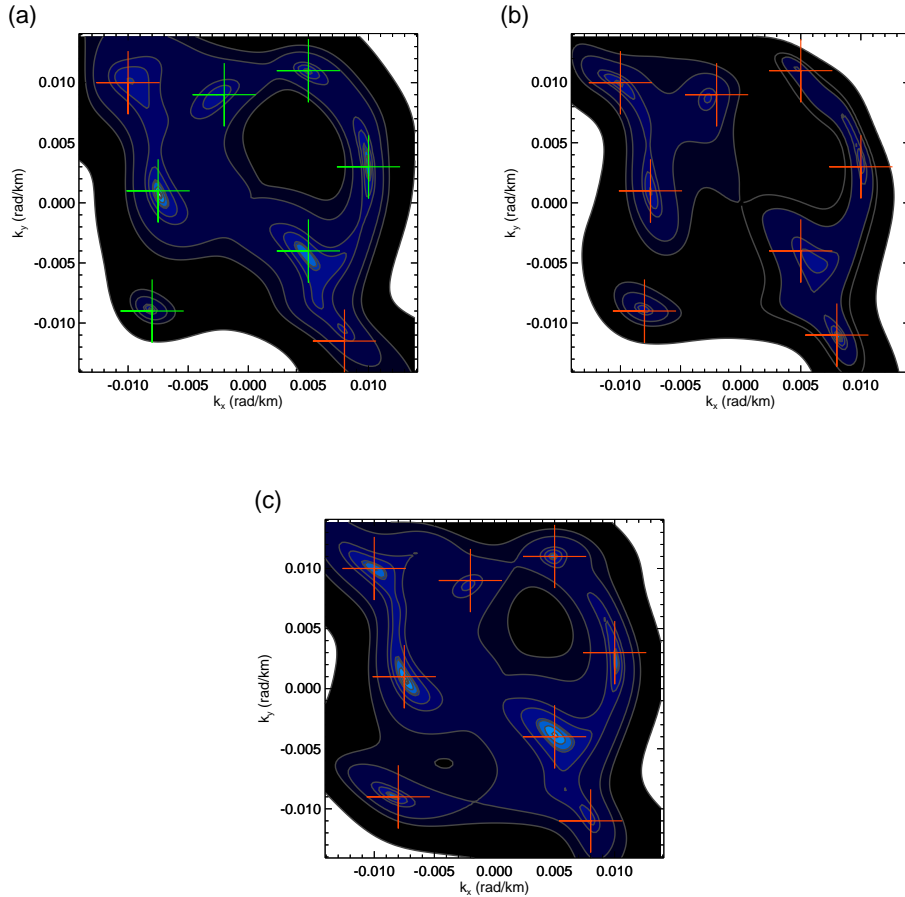
Figure 4. Estimated $P(\omega, \boldsymbol{k})$ for **(a)** six random-phase plane waves (green crosses) and two coherent structures (red crosses), **(b)** eight coherent structures ($\lambda = 1000$, $d = 250$ in both cases) and **(c)** eight coherent structures (Gaussian modulated wave packets). The contours denote the same relative powers as in Fig. 3.

The final cases to be tested will consist of various combinations of structure-like signals and random-phase plane waves.

To model the advection of coherent structures past the spacecraft, we define them as having a characteristic mean radius d and a mean spacing between them λ as shown in Fig. 1. Both of these parameters vary with Poisson statistics about a mean for each structure advected over the spacecraft. It is important to note for Poisson statistics that the mean and the variance are equal. The fluctuations due to the structure can be thought of as a "wave packet"; these fluctuations have a mean distance and separation, d and λ. The fluctuations themselves are defined as plane waves (Eq. 7), each wave packet always begins at the same phase, and only the specific d and λ are random. One typical time series for a series of structures being convected across the spacecraft is shown in Fig. 2a. We can also investigate the case for when the fluctuations are modulated by a Gaussian envelope, which would make the fluctuations stronger closer to the centre, which is the case with coherent structures such as the MHD Alfvén vortex (Petviashvili and Pokhotelov, 1992;

Alexandrova et al., 2006; Alexandrova, 2008). This scenario is shown in Fig. 2b.

The total signal is given by the summation of the i individual components, where the summation can contain components that are random (or non-random) phase plane waves or coherent structures.

The requirement of the k-filtering technique that waves have random phases is illustrated here. For instance, two waves similar to those in Eq. (7) are given by $\sin(\boldsymbol{k}_1 \cdot \boldsymbol{r} - \omega_1 t - \phi_1)$ and $\sin(\boldsymbol{k}_2 \cdot \boldsymbol{r} - \omega_1 t - \phi_2)$; the combined wave field will be

$$2 \sin\left[\frac{(\boldsymbol{k}_1 + \boldsymbol{k}_2) \cdot \boldsymbol{r} - 2\omega_1 t - (\phi_1 + \phi_2)}{2}\right]$$
$$\times \cos\left[\frac{(\boldsymbol{k}_1 - \boldsymbol{k}_2) - (\phi_1 - \phi_2)}{2}\right]. \tag{8}$$

If $\phi_1 - \phi_2$ is fixed (the two waves are coherent), then the above equation basically produces a new wave field with a wave vector at $(\boldsymbol{k}_1 + \boldsymbol{k}_2)/2$ at the same frequency ω_1, very different from the original two waves. However, if $\phi_1 - \phi_2$
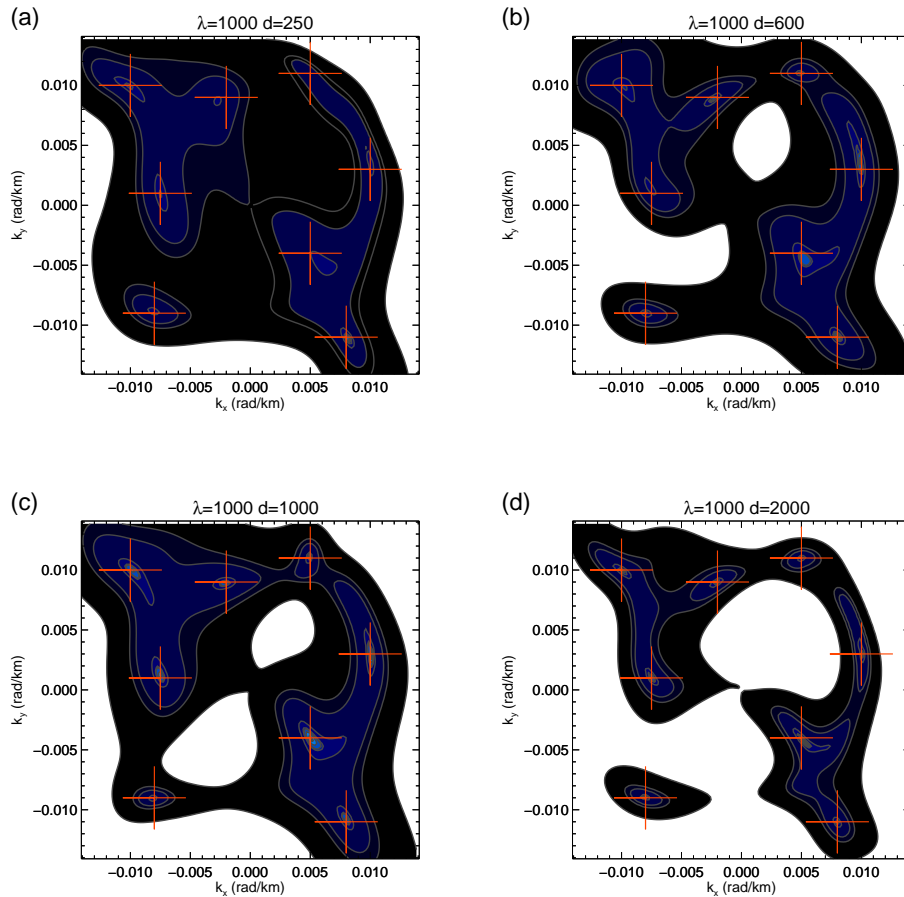
Figure 5. Estimated $P(\omega, \boldsymbol{k})$ for eight coherent structures for a variety of ratios of d/λ. Note that the estimation is broadened as the d becomes very small relative to λ. The contours denote the same as in Fig. 3.

is randomised (at each wave period), the ensemble average of the k-filtering technique will recover the two original random-phase waves.

4   Results

The results for the case of random and non-random plane waves are shown in Fig. 3, where the green crosses denote the random-phase plane waves and the red the non-random components; the contours denote the estimation $P(\omega, \boldsymbol{k})$ from k filtering. Note that, mathematically, the power of an individual wave is a singular point located at the crosses. As can be seen, the method can easily recover eight random plane waves, and when we introduce one non-random wave the method can recover both random and non-random components. However, when more than one component in the time series is non-random, k filtering has difficulty resolving the non-random fluctuations. This is due to the requirement of random phases, since two or more waves (of the same frequency) with fixed-phase differences will superpose, which will result in a periodic resultant amplitude. In pre-

vious tests of the method, the need for incoherent signals was recognised (Capon, 1969; Pinçon and Lefeuvre, 1991; Motschmann et al., 1998). A key point is that recovery of random-phase components is *unaffected* by the presence of non-random components in the time series. This result gives confidence that, provided that the phases of some waves are random, the method can recover the random component.

Following this test we now seek to understand the effects that intermittent coherent structures have on the estimation of $P(\omega, \boldsymbol{k})$. We introduce some structure elements into the signal as shown in Fig. 2. Figure 4a shows the cases where we have a combination of random-phase plane waves (green) and coherent structures (red). The method succeeds in identifying all components of the defined signal, alleviating the issues which were pointed out by Roberts et al. (2013). Figure 4b shows a case where the signal contains only coherent structures, while Fig. 4c shows the case where the structures are modulated with a Gaussian. We note that while the technique can identify all of the structures present, the estimation $P(\omega, \boldsymbol{k})$ is broadened in wave space. This implies that the errors associated with a signal consisting mainly of coherent structures are larger than when the signal only consists of

random-phase plane waves. We also note that there is very little difference in the estimation of $P(\omega, \boldsymbol{k})$ when we modulate the structures using a Gaussian function, as was demonstrated in Fig. 2b.

To explore the issue of broadening associated with a signal composed of structures, we investigate the choice of the structure parameters λ and d, and what effects these have on the estimation from k filtering. If $d \gg \lambda$, a structure and a random-phase plane wave will produce very similar fluctuations as seen by the satellite. Figure 5 shows the power spectral density $P(\omega, \boldsymbol{k})$ for various values of λ and d. A salient feature of these plots is that the estimation improves (contours are closer together) when $d \ll \lambda$, and declines as $\lambda \gg d$, but the peaks in all cases correspond well to where the structures are launched in k space. We suggest that a reasonable limit for k filtering to be able to resolve these structures is that $d/\lambda \geq 0.1$. When λ becomes very large there will be fewer structures present in a given interval. The necessary statistics required for the ensemble average of the k-filtering technique will not be met for such a interval. On the other hand, as d increases the structures will be similar to non-random-phase waves, and cannot be identified as we have discussed at the end of Sect. 3. These criteria are often met in space plasmas, for example, in the Earth's magnetosheath (Alexandrova et al., 2006; Alexandrova, 2008), where Alfvénic vortices were identified and the parameters d and λ were derived from their spectral shapes, and were shown to be approximately $d = 600$ km and $\lambda = 1000$ km respectively.

5 Conclusions

By investigating synthetic magnetic field data we have demonstrated that the k-filtering technique can be used to analyse a signal which consists of random-phase plane waves and coherent structures. The presence of any non-random plane wave *does not* affect the ability to resolve random-phase components, and can even resolve a random component when it is a minority. In the limit $d \gg \lambda$, there is very little difference between the wave and the structure paradigm and k filtering has no difficulty in resolving structures in this limit. As $\lambda \gg d$, the estimation of $P(\omega, \boldsymbol{k})$ is broadened, making errors in estimating $\boldsymbol{k}$ larger. We have also tested for a signal where the parameters are similar to those observed in the Earth's magnetosheath, and the method resolves the structures with comparable accuracy to the random-phase plane wave case. We have demonstrated that waves at any frequency are required to be incoherent, since the k-filtering technique is unable to resolve two waves with a fixed-phase difference. Nevertheless a series of randomly located coherent structures arranged with characteristic mean radius and spacing can be assumed to be incoherent and can be resolved by means of the k-filtering technique. While they are "coherent" within their radius,

they are incoherent with respect to each other due to their random locations. For turbulent environments such as the solar wind, where waves and structures are both present, the incoherency of the signal is likely to be satisfied, and the application of the technique justified. We conclude that there should be no issues in using this technique on a signal which contains both random phases and non-random phases.

Edited by: L. Vazquez

References

Alexandrova, O.: Solar wind vs magnetosheath turbulence and Alfvén vortices, Nonlin. Processes Geophys., 15, 95–108, doi:10.5194/npg-15-95-2008, 2008.

Alexandrova, O., Mangeney, A., Maksimovic, M., Cornilleau-Wehrlin, N., Bosqued, J.-M., and André, M.: Alfvén vortex filaments observed in magnetosheath downstream of a quasi-perpendicular bow shock, J. Geophys. Res., 111, A12208, doi:10.1029/2006JA011934, 2006.

Balogh, A., Carr, C. M., Acuña, M. H., Dunlop, M. W., Beek, T. J., Brown, P., Fornacon, K.-H., Georgescu, E., Glassmeier, K.-H., Harris, J., Musmann, G., Oddy, T., and Schwingenschuh, K.: The Cluster Magnetic Field Investigation: overview of in-flight performance and initial results, Ann. Geophys., 19, 1207–1217, doi:10.5194/angeo-19-1207-2001, 2001.

Burlaga, L. F. and Ogilvie, K. W.: Magnetic and thermal pressure in the solar wind, Sol. Phys., 15, 61–71, 1970.

Capon, J.: High-resolution frequency-wavenumber spectrum analysis, Proc. IEEE, 57, 1408–1418, doi:10.1109/PROC.1969.7278, 1969.

Eastwood, J. P., Balogh, A., Lucek, E. A., Mazelle, C., and Dandouras, I.: On the existence of Alfvén waves in the terrestrial foreshock, Ann. Geophys., 21, 1457–1465, doi:10.5194/angeo-21-1457-2003, 2003.

Escoubet, C. P., Fehringer, M., and Goldstein, M.: *Introduction* The Cluster mission, Ann. Geophys., 19, 1197–1200, doi:10.5194/angeo-19-1197-2001, 2001.

Ghosh, S., Thomson, D. J., Matthaeus, W. H., and Lanzerotti, L. J.: Coexistence of turbulence and discrete modes in the solar wind, J. Geophys. Res., 114, A08106, doi:10.1029/2009JA014092, 2009.

Glassmeier, K.-H., Motschmann, U., Dunlop, M., Balogh, A., Acuña, M. H., Carr, C., Musmann, G., Fornaçon, K.-H., Schweda, K., Vogt, J., Georgescu, E., and Buchert, S.: Cluster as a wave telescope – first results from the fluxgate magnetometer, Ann. Geophys., 19, 1439–1447, doi:10.5194/angeo-19-1439-2001, 2001.

Jian, L. K., Russell, C. T., Luhmann, J. G., Strangeway, R. J., Leisner, J. S., and Galvin, A. B.: Cyclotron Waves in the Solar Wind Observed By Stereo Near 1 Au, Astrophys. J., 701, L105–L109, 2009.

Jian, L. K., Russell, C. T., Luhmann, J. G., Anderson, B. J., Boardsen, S. A., Strangeway, R. J., Cowee, M. M., and Wennmacher, A.: Observations of ion cyclotron waves in the solar wind near 0.3 AU, J. Geophys. Res., 115, A12115, doi:10.1029/2010JA015737, 2010.

Motschmann, U.: Wavelength and direction filtering by magnetic measurements at satellite arrays: generalized minimum variance analysis, J. Geophys. Res., 101, 4961–4966, doi:10.1029/95JA03471, 1996.

Motschmann, U., Glassmeier, K. H., and Pincon, J. L.: Multispacecraft filtering: Plasma mode recognition, in: Analysis Methods for Multi-Spacecraft Data, ESA Publications Division, Noordwijk, the Netherlands, 1998.

Narita, Y., Glassmeier, K.-H., and Motschmann, U.: High-resolution wave number spectrum using multi-point measurements in space – the Multi-point Signal Resonator (MSR) technique, Ann. Geophys., 29, 351–360, doi:10.5194/angeo-29-351-2011, 2011.

Neubauer, F. M. and Glassmeier, K. H.: Use of an array of satellites as a wave telescope, J. Geophys. Res., 95, 19115–19122, doi:10.1029/JA095iA11p19115, 1990.

Petviashvili, V. I. and Pokhotelov, O. A.: Dipole Alfvén vortices, JETP Lett., 42, 54–56, 1985.

Petviashvili, V. I. and Pokhotelov, O. A.: Solitary Waves in Plasmas and in the Atmosphere, Gordon and Breach Science Pub., Philadelphia, PA, 1992.

Pinçon, J. L. and Lefeuvre, F.: Local characterization of homogeneous turbulence in a space plasma from simultaneous measurements of field components at several points in space, J. Geophys. Res., 96, 1789–1802, 1991.

Pinçon, J. L. and Lefeuvre, F.: The application of the generalized Capon method to the analysis of a turbulent field in space plasma: Experimental constraints, J. Atmos Terr. Phy., 54, 1237–1247, 1992.

Pinçon, J. L. and Motschmann, U.: Multi spacecraft filtering: general framework, in: Analysis Methods for Multi-Spacecraft Data, edited by: Paschmann, G. and Daly, P. W., ESA Publications Division, Noordwijk, the Netherlands, 1998.

Robert, P., Roux, A., Harvey, C., Dunlop, M., Daly, P., and Glassmeier, K. H.: Tetrahedron geometric factors, in: Analysis Methods for Multi-Spacecraft Data, Chap. 13, edited by: Paschmann, G. and Daly, P., ESA Publications Division, Noordwijk, the Netherlands, 323–348, 1998.

Roberts, O. W., Li, X., and Li, B.: Kinetic plasma turbulence in the fast solar wind measured by cluster, Astrophys. J., 58, 1–8, 2013.

Sahraoui, F., Pincon, J. L., Belmont, G., Rezeau, L., Cornilleau-Wehrlin, N., Robert, P., Mellul, L., Bosqued, J. M., Balogh, A., Canu, P., and Chanteur, G.: ULF wave identification in the magnetosheath: the k-filtering technique applied to Cluster II data, J. Geophys. Res., 108, 1–19, 2003.

Sahraoui, F., Belmont, G., Pinçon, J. L., Rezeau, L., Balogh, A., Robert, P., and Cornilleau-Wehrlin, N.: Magnetic turbulent spectra in the magnetosheath: new insights, Ann. Geophys., 22, 2283–2288, doi:10.5194/angeo-22-2283-2004, 2004.

Sahraoui, F., Belmont, G., Rezeau, L., Cornilleau-Wehrlin, N., Pinçon, J., and Balogh, A.: Anisotropic turbulent spectra in the terrestrial magnetosheath as seen by the cluster spacecraft, Phys. Rev. Lett., 96, 075002, doi:10.1103/PhysRevLett.96.075002, 2006.

Sahraoui, F., Belmont, G., Goldstein, M. L., and Rezeau, L.: Limitations of multispacecraft data techniques in measuring wave number spectra of space plasma turbulence, J. Geophys. Res., 115, 1–10, 2010.

Taylor, G. I.: The spectrum of turbulence, P. Roy. Soc. A, 164, 476–490, 1938.

Tjulin, A., Pinçon, J.-L., Sahraoui, F., Andre, M., and Cornilleau-Wehrlin, N.: The k-filtering technique applied to wave electric and magnetic field measurements from the Cluster satellites, J. Geophys. Res., 110, 1–17, 2005.

Tjulin, A., Lucek, E. A., and Dandouras, I.: Wave activity inside hot flow anomaly cavities, J. Geophys. Res., 113, A08113, doi:10.1029/2005JA011125, 2008.